VILNIUS TECH
Vilnius Gediminas Technical University

AVIATION
ISSN: 1648-7788 / eISSN: 1822-4180
2022 Volume 26 Issue 4: 224–234
https://doi.org/10.3846/aviation.2022.17552

THE EFFECT OF MOTION FORMATION ON COOPERATIVE NAVIGATION

Mohammad SABERI TAVAKKOLI, Ghasem KAHE *, Fatemeh SADEGHIKIA

Aerospace Research Institute, Tehran, Iran

Received 5 April 2021; accepted 3 November 2021

Abstract. The effect of formation movement on the performance of cooperative navigation is investigated in this paper. First, the inertial navigation system of each agent with a certain accuracy is modeled and simulated. Initial results showed that the navigation error of each agent increased individually over time, and this problem is more severe for agents equipped with a weaker system. Cooperative navigation is implemented for the agents to resolve this problem. It is shown that the total navigation errors are improved by observing and participating the relative distance between the agents. Various simulations and experimental tests using two real agents supported this assertation. The performance of cooperative navigation can be improved further through appropriate formation. Proper formations are investigated and evaluated through simulations. The collective covariance matrix is employed to form an objective function using an extended Kalman filter (EKF). This function has been minimized using Newton's method, which could be the solution for the formation. The simulation results show that better accuracy can be achieved by applying the optimal formation trajectory.

Keywords: navigation, cooperative navigation, extended Kalman Filter, EKF, CNS, formation.

Introduction

Navigation systems are essential vehicle subsystems, such as Unmanned Aerial Vehicle (AUVs), land mobile robots, aircrafts, UAVs, satellites, or spacecrafts. Different navigation systems are used according to the requirements of each vehicle, mission, and the environment. Inertial navigation systems, radio navigation systems, and other types of systems have grown significantly throughout recent years. The navigation systems using MEMS[1] technology have been prevalent because they are relatively accurate, lightweight, and inexpensive.

There are several ways to increase the accuracy of navigation systems. Generally, either an expensive equipment with highly accurate sensors is used (such as INS[2] with high-precision accelerometer and gyros or celestial navigation systems), or an integration of several navigation systems is utilized as auxiliary or alternative navigation systems (such as INS/GPS integration or using two INSs at the same time).

Sometimes using aided navigation systems will increase the cost. Therefore, to reduce the cost, inter-agent navigation is has been used in many types of research, which have been related to ground robots, naval and submarine vehicles, aerial vehicles such as drones, and space vehicles such as satellites and spacecrafts. They all have in common some sensors that measure relative variables such as relative distance, relative orientation, relative position, and relative velocity. For example, in some of the previous studeis, relative navigation is considered between two satellites, in one of them, UHF waves, and in the other, X-rays are emitted in the galaxy. These waves have been used to obtain relative navigation, which eventually resulted in an accuracy of 0.5 m in relative position and 1 cm/s in relative velocity (Montenbruck et al., 2002; Sheikh et al., 2007; Martin, 2011). Cutler et al. (2013) refer to the indoor navigation of the quadrotor, which uses an integration with IR[3] data due to the low inertial navigation accuracy of these drones. The drone can measure both range and bearing from the markers in the environment. Accurate relative navigation is also performed via laser equipment (Lee et al., 2018). In the relative navigation algorithm, the estimations are through EKF and Unscented Kalman Filter (UKF), and this paper also compares the two filters. In the simulations, sometimes EKF gives inaccurate answers or leads to divergence,

[1] Micro-ElectroMechanical System

[2] Inertial Navigation System

[3] Infrared

*Corresponding author. E-mail: *kahe@ari.ac.ir*

while UKF doesn't have these problems. In a PhD thesis from Nanyang Technological University, the formation of drones in GPS-denied is discussed (Guo, 2018). This thesis states that UWB radio frequency technology can compensate for the lack of access to GPS. The first step in this thesis is to localize UAVs based on UWB. It is done by measuring the distance between drones and radio transmitters fixed in the operating space. In the next step, using a landmark makes it possible for each drone to estimate its relative distance from that marker to correct its global position. Another challenge raised in this thesis is obtaining a relative position among quadcopters for which there is no specific commercial equipment, and the author must obtain the relative position of the agents using the two afore-mentioned steps. Rutkowski et al. (2016) present a path planning method to reduce the uncertainty of two autonomous cars moving from a known position to the desired location.

In this case, an odometer is mounted on each car to detect changes in the position and heading. The cars also have a sensor that can measure the relative distance between them. Cooperative navigation is also used to reduce road and city traffic. Summerfield et al. (2020) develope a cooperative centralized routing algorithm that minimizes the whole network congestion. In this algorithm, a heuristic cooperative routing algorithm is taken, which minimizes the network congestion. In another study, Mokhtarzadeh and Gebre-Egziabher (2016) improve the navigation accuracy by sharing navigation data in a GPS-denied environment. This article studies UAVs, which have AHRS[4] and Airspeed DR[5] sensors, and finally uses flight test data from a reference to prove its work.

Cooperative navigation also works in human-robot environments. A robot needs to predict human trajectories and plan its own trajectory correspondingly in the same shared space to meet comparable human efficiency. Khambhaita and Alami (2019) present a navigation planner that can plan such cooperative trajectories, while simultaneously enforces the robot's kinematic constraints and avoid other non-human dynamic obstacles. Using robust social constraints of projected time to a possible future collision, compatibility of human-robot motion direction, and proxemics, the planner can replicate human-like navigation behavior not only in open spaces but also in confined areas. In another article, Cooperative Vision-and-Dialog Navigation is presented (Thomason et al., 2020). In this study, a dataset of over 2k embodied human-human dialogs were situated in simulated photorealistic home environments. It is a kind of cooperative navigation that needs a human voice. The Navigator asks his partner, the Oracle, who has privileged access to the best next steps the Navigator should take according to the shortest path planner. Finding a safe path to navigate in the environments crowded with humans is a challenge.

In a series of articles published in three consecutive years, the navigation accuracy of a quadrotor called "boy" in the urban environment is investigated (Vetrella et al., 2016, 2017; Causa et al., 2018). Due to the existence of tall buildings, this quadrotor could not access GNSS satellites. Therefore, some other quadcopters called "Father", which fly at high altitudes and have free access to GPS satellites, are used to increase the accuracy of the navigation of the son. The communication between the father/fathers and the son is used to improve the son's navigation performance since the father/fathers has sensors that measure the relative information between himself and the son and provides it to the son after processing, so he has the ability to correct his position. In the study conducted by Causa et al. (2018) the relative measurements and information sharing between the father and son are the primary fundations of this integration algorithm. Different filtering architectures in relative measurements focusing on measurement equations and relative covariance matrices are examined in this paper. The Dilution of Precision (DOP) concept is used to predict the accuracy of a boy's position due to the availability of GNSS and relative measurements, which uses this criterion to achieve an optimal geometry to improve his navigation performance. Experimental data has shown how proper geometry can help visual cooperation in navigation by achieving meter accuracy in long-time flights. In another article, a similar issue with references (Vetrella et al., 2016, 2017; Causa et al., 2018) is dealt with. However, instead of using auxiliary quadrotor(s), a ground robot is used (Sivaneri & Gross, 2017). This article deals with cooperative navigation between UAVs and UGV[6]s that operate in GPS-challenged environments; therefore, the focus is on designing the optimal UGV motion to work best to assist UAV navigation. The UGV location is chosen to provide the best navigation assistance to the UAV. Using these methods in the natural environment has been shown to improve the error from 1 m to 10 cm. In another article, the same issue is addressed again with references (Vetrella et al., 2016, 2017; Causa et al., 2018), but this time the GPS-challenge has arisen due to the flight of a quadrotor in the valley (Cledat & Cucci, 2017). In this article, two UAVs are considered; one is flying over a valley with access to GNSS signals and can see the other drone flying in the middle of the valley and does not have access to GNSS signals. The upper drone can track and control the drone in the valley via a camera, ultimately increasing its positioning accuracy.

For many years, one of the topics has been formation flying and its effect on relative navigation accuracy, called cooperative navigation system or CNS. This type of navigation contributes to both individual and collective agent navigation. In cooperative navigation, collective estimation is always better than individual estimation (Sanderson, 1998). Sanderson (1998) discusses cooperative navigation

[4] Attitude and Heading Reference Systems

[5] Dead-Reckoning

[6] Unmanned Ground Vehicle

for robots, which ultimately leads to a better estimate of collective navigation by increasing the relative navigation accuracy. In this paper, the relative distance measurement is considered as the Kalman filter's input to have a better collective position estimation. It is also noted that as the number of robots increases, the accuracy of collective estimation will increase too. Each robot uses only the relative distance information between itself and other robots, and the relative distance information between other robots does not affect it. The effect of CNS is in a way that if the accuracy of one robot is high, it will increase the accuracy of the position estimation in other robots as well. In a research done by Fosbury and Crassidis (2008), complete equations of motion in aerial navigation for formation flying with a leader and its follower perspective are presented. In this paper, EKF is used to estimate the relative position between two vehicles. The variable states of the leader are assumed to be known, while the relative variable states are estimated by measuring the line of sight (LOS) between the two vehicles and the acceleration and angular velocity of the leader.

Optimal control theory has also been used to minimize a criterion according to the type of sensors. This criterion prevents too many maneuvers for the follower. During the cooperative flight, the UAV's swarm can use the received position and ranging information of the adjacent UAV to calculate the position and fuse it with its sensor position information. The final positioning accuracy depends not only on the capability of the ranging sensor but also on the position accuracy and formation of the adjacent UAV (Chen et al., 2020). An article used integrated video navigation and GPS/VISNAV (Chen et al., 2010). The integration is used to achieve high accuracy in relative navigation and determine the formation flying of the closest spacecraft. In the proposed integration, the federated Kalman filter (FK) is used. In another article by the same authors, the GPS/VISNAV integration is used again, but this time to improve the accuracy and performance of fault tolerance in relative navigation and with the purpose of determining the position for the formation of very close satellites (Wang, 2011; Wang et al., 2011a, 2011b).

Sometimes, agents have different observations of the same phenomenon, leading to a more accurate observation by sharing their observations. For example, Hong and Simon (2017) found that several agents have different estimates of a target space that try to estimate the target better by sharing their estimates. In this research, which has a leader-follow formation flight strategy, the Hill-Clohessy-Wiltshire (HCW) equations are used for relative navigation. Vetrella et al. (2018) considered cooperative navigation to estimate the main agent's attitude with the help of other agents reliably and accurately. It is done through tight integration in the extended Kalman filter so that the data of the GNSS receivers and the visual system be integrated with the data of the inertial sensors and magnetometer. The main idea is to determine the attitude of the main agent using the difference between the data of the GNSS receivers, and the visual system of the other agents instead of using multiple GNSS antennas. In another article, using cooperative navigation reduced the growth of dead reckoning navigation error in ground robots (Roumeliotis & Bekey, 2002). The dead-reckoning navigation used in this article is achieved by rotating the wheels. Robots only move in the longitudinal body axis and can have a side angle that makes the equations of motion a little easier. Robots are assumed to use the relative distance and relative angle to reduce navigation error. This relative data is used when two robots are at a minimum detectable distance from each other. This paper proves that the growth of dead reckoning navigation error is reduced when cooperative navigation is used. Faghihinia et al. (2021) investigated the propagation of uncertainty in a cooperative navigation algorithm (CNA) for a group of flying robots (FRs). For further studies, a relaxed analytical performance index through a closed-form solution is derived. Moreover, the effects of the sensors' noise covariance and the number of FRs on the growth rate of the position error covariance are investigated. Analytically, it is shown that the covariance of position error in the vehicles equipped with the Inertial Measurement Unit (IMU) is proportional to the cube of time.

Cooperative navigation also works in unknown places. Jin et al. (2019) addressed a multi-agent cooperative navigation problem that multiple agents work together in an unknown environment to reach different targets without collision and minimize the maximum navigation time they need. To this end, they have modeled the navigation policy as a combination of a dynamic target selection policy and a collision avoidance policy. Since these two policies are coupled, an interlaced deep reinforcement learning method is proposed to learn them simultaneously.

A review of previous research shows that most references face some common challenges, including the growth error in navigation systems. To overcome these challenges integrated navigation and sometimes relative measurements are used. Another challenge that has been addressed in some cases is the GNSS-challenge. This challenge results from the fact that most robots use GNSS receivers, especially GPS, which have many problems. Therefore, the idea implemented in this article is to eliminate satellite navigation aids and increase the accuracy of cooperative navigation through the optimal formation of agents.

1. Description of the problem

As in previous studies, authors seek to reduce navigation error and address the challenges posed by using cooperative navigation. The main purpose of this research work is to achieve the best inter-agent formation so that the cooperative navigation error is minimized without the use of aided navigation equipment such as GPS. This article

claims that it is possible to experience up to a 40% increase in the accuracy of cooperative navigation in a group of agents by using the optimal formation. This formation can be in a group flight at a constant altitude from one position to another, in which each agent, in addition to navigating itself, can also help improve the navigation performance of other agents. The relative data that will be measured between the agents is the relative distance.

Another point to be made is that to achieve good relative data, at least one agent must have more accurate navigation. This increase in accuracy is either due to more accurate equipment or several landmarks.

2. Equations of motion

As mentioned, agents have freedom of movement in a two-dimensional (2D) space. It is a three-degree of freedom (3DOF) of movement, which includes moving in the lateral and longitudinal directions and changing the heading angle. Five variable states are considered for such dynamics including: two displacements, two linear velocities, and a heading angle φ.

$$\vec{X} = \begin{bmatrix} \varphi & v_x & v_y & x & y \end{bmatrix}^T . \tag{1}$$

Moreover, the state-space equations for the variables are defined as the following equation:

$$\dot{\vec{X}} = \begin{bmatrix} \omega & a_x - \omega v_y & a_y + \omega v_x & v_x & v_y \end{bmatrix}^T , \tag{2}$$

where ω is angular velocity about the axis perpendicular to the x – y plane; and a_x and a_y are acceleration in the x and y directions. Since the agents use an inertial navigation system instead of accelerations and angular velocity, the output of the accelerometers and gyro are substituted in the above equations.

3. Extended Kalman Filter

Assuming that a discrete EKF is used to integrate the data, the following equations can be assumed:

$$x_k = f\left(x_{k-1}, u_k\right) + w_k ; \tag{3}$$

$$z_k = h\left(x_k\right) + \upsilon_k , \tag{4}$$

where w_k and υ_k are process noise and measurement noise, respectively, which are assumed to be the Gaussian noise with zero mean and covariances Q_k and R_k. Furtheremore u_k is regarded as the control of the system. f is a function that calculates the estimation of system states based on the previous estimation, and similarly h is a function that estimates the measurement based on the previous measurement. These two functions cannot directly have a covariance matrix and must use partial derivatives (or Jacobin) at any step times. According to the assumptions, the EKF algorithm will be as the equations are shown in Table 1 (Noureldin et al., 2013):

Table 1. EKF algorithm

Predict		
Predicted State Estimate	$\hat{x}_{k\|k-1} = f\left(\hat{x}_{k-1\|k-1}, u_k\right)$	(5)
Predicted Covariance Estimate	$P_{k\|k-1} = F_k P_{k-1\|k-1} F_k^T + G_k Q_k G_k^T$	(6)
Update		
Innovation or Measurement Residual	$\tilde{y}_k = z_k - h\left(\hat{x}_{k\|k-1}\right)$	(7)
Innovation (or Residual) Covariance	$S_k = H_k P_{k\|k-1} H_k^T R_k$	(8)
Near-Optimal Kalman Gain	$K_k = P_{k\|k-1} H_k^T S_k^{-1}$	(9)
Updated State Estimate	$\hat{x}_{k\|k} = \hat{x}_{k\|k-1} + K_k \tilde{y}_k$	(10)
Updated Covariance Estimate	$P_{k\|k} = \left(I - K_k H_k\right) P_{k\|k-1}$	(11)

where Q_k is system noise covariance,R_k measurement noise covariance and F_k, G_k and H_k are obtained as follows:

$$F_k = I + A_k dt \quad , \quad G_k = B_k dt \quad , \quad H_k = \left.\frac{\partial h}{\partial x}\right|_{\hat{x}_{k|k-1}} , \tag{12}$$

where I is an identity matrix in the same dimension of the problem, and A_k and B_k are Jacobins of state-space equations with respect to state variables and input variables which were obtained as the following equations:

$$A_k = \left.\frac{\partial f}{\partial x}\right|_{\hat{x}_{k-1|k-1}, u_k} \quad , \quad B_k = \left.\frac{\partial f}{\partial u}\right|_{\hat{x}_{k-1|k-1}, u_k} . \tag{13}$$

If x is the state vector, z_{rel} is the observation of the relative state vector between two or more agents, x_{nav} is the navigation system state vector, and the integration of relative and absolute navigation data is desirable to increase the accuracy of integrated navigation, based on Equations (3) to (13), the following equations will be derived:

$$\hat{x}_{nav(k|k)} = \hat{x}_{(k|k-1)} + \underbrace{\left(P_{(k|k-1)} H_{(k)}^T \left(\underbrace{H_{(k)} P_{(k|k-1)} H_{(k)}^T R_{(k)}}_{S_k} \right) \right)}_{K_k} \underbrace{\left(z_{rel(k)} - h_{rel}\left(\hat{x}_{(k|k-1)}\right) \right)}_{\tilde{y}_k} . \tag{14}$$

In Eq. (14) $h_{rel}\left(\hat{x}_{(k|k-1)}\right)$ is a function used to predict the relative state vector. Therefore, it is observed that the navigation data is related to the relative state vector via this function.

The only observation is the relative distance. Since relative distance is not the state variable of the system, its relations must be derived as follows:

$$h_{rel}\left(\hat{x}_{(k|k-1)}\right)=\sqrt{\left(x_i-x_j\right)^2+\left(y_i-y_j\right)^2}\ . \tag{15}$$

Therefore, the observation matrix according to Equation (12) will be formed as follows:

$$\mathrm{H}_{CNS}=\begin{bmatrix} & & & & & & & & & & & & \\ 0&0&0&\dot{h}_{x12}&\dot{h}_{y12}&0&0&0&-\dot{h}_{x12}&-\dot{h}_{y12}&0&0&0&0&0\\ 0&0&0&\dot{h}_{x13}&\dot{h}_{y13}&0&0&0&0&0&0&0&0&-\dot{h}_{x13}&-\dot{h}_{y13}\\ 0&0&0&-\dot{h}_{x21}&-\dot{h}_{y21}&0&0&0&\dot{h}_{x21}&\dot{h}_{y21}&0&0&0&0&0\\ 0&0&0&0&0&0&0&0&\dot{h}_{x23}&\dot{h}_{y23}&0&0&0&-\dot{h}_{x23}&-\dot{h}_{y23}\\ 0&0&0&-\dot{h}_{x31}&-\dot{h}_{y31}&0&0&0&0&0&0&0&0&\dot{h}_{x31}&\dot{h}_{y31}\\ & & &0&0&0&0&0&-\dot{h}_{x32}&-\dot{h}_{y32}&0&0&0&\dot{h}_{x32}&\dot{h}_{y32}\end{bmatrix}, \tag{16}$$

where:

$$\dot{h}_{xij}=\frac{\Delta xij}{\sqrt{\left(x_i-x_j\right)^2+\left(y_i-y_j\right)^2}},$$

$$\dot{h}_{yij}=\frac{\Delta yij}{\sqrt{\left(x_i-x_j\right)^2+\left(y_i-y_j\right)^2}}. \tag{17}$$

4. Cooperative navigation equation

This paper assumes that the agents use a micro-electromechanical system (MEMS) for navigation, and the relative observations are the only data for integration. The relative distance is the data to integrate. One of the cooperative navigation methods is using the total error covariance matrix as follows (Roumeliotis & Bekey, 2002):

$$P_{CNS}=\begin{bmatrix}P_{11}&P_{12}&P_{13}\\P_{21}&P_{22}&P_{23}\\P_{31}&P_{32}&P_{33}\end{bmatrix}, \tag{18}$$

where P_{ii} is the covariance matrix of ith agent and P_{ij} is the cooperative covariance matrix between the ith and jth agents. The values of the main diagonal elements of the matrix P_{CNS} or P_{ii} are obtained in the prediction phase according to Equation (6), but cooperative elements, i.e.P_{ij}, are obtained from the following equation:

$$P_{ij}^{+}=F_iP_{ij}^{-}F_j^T\ . \tag{19}$$

The first step is considering a zero matrix with its values. In the update steps, the matrix P_{CNS} is also updated via Equation (11). When the agents do not meet each other, or the relative data is not been observed, the non-diagonal elements will be obtained from the following equation, which will not affect the cooperative navigation (Roumeliotis & Bekey, 2002).

$$P_i^{+}=F_i\sqrt{P_{ij}^{-}}\quad,\quad P_i^{-}=\sqrt{P_{ij}^{-}}F_j^T\ . \tag{20}$$

Equation (20) will be valid until a relative observation occurs and enters the integration.

5. Optimal formation equations

In this section, the goal is to achieve equations that make cooperative navigation accuracy as a function of formation. Therefore, the best variable representing the accuracy of cooperative navigation is the total error covariance matrix. Using the concept of determinant or trace of this matrix can be a good criterion for evaluation. The lower the two values are, the higher the navigation accuracy will be. Therefore, an equation should be looked for that minimizes the determinant or trace of total error covariance matrix by changing the formation geometry between the agents. Newton's method is used for this purpose. Newton's method is based on gradient and hessian that in each step can obtain the best solution of the next step for the variable states. Substituting Equations (7), (8), and (9) in Equation (11), the covariance error matrix for each factor can be written as follows:

$$P_{k|k}=\left(F_kP_{k-1|k-1}F_k^T+G_kQ_kG_k^T\right)-\ldots$$
$$\left(F_kP_{k-1|k-1}F_k^T+G_kQ_kG_k^T\right)H_k^T\left(H_k\left(F_kP_{k-1|k-1}F_k^T+G_kQ_kG_k^T\right)H_k^T+R_k\right)^{-1}$$
$$H_k\left(F_kP_{k-1|k-1}F_k^T+G_kQ_kG_k^T\right). \tag{21}$$

By substituting Equations (12) and (13), an equation is formed in which the error covariance matrix will be a function of the agents' positions, which is specified in the following equation:

$$P_{k|k}=\begin{pmatrix}\left(I+\left.\frac{\partial f}{\partial x}\right|_{\hat{x}_{k-1|k-1},u_k}dt\right)P_{k-1|k-1}\left(I+\left.\frac{\partial f}{\partial x}\right|_{\hat{x}_{k-1|k-1},u_k}dt\right)^T+\\ \left(\left.\frac{\partial f}{\partial u}\right|_{\hat{x}_{k-1|k-1},u_k}dt\right)Q_k\left(\left.\frac{\partial f}{\partial u}\right|_{\hat{x}_{k-1|k-1},u_k}dt\right)^T\end{pmatrix}\ldots$$

$$-\left(\begin{pmatrix}\left(I+\left.\frac{\partial f}{\partial x}\right|_{\hat{x}_{k-1|k-1},u_k}dt\right)P_{k-1|k-1}\left(I+\left.\frac{\partial f}{\partial x}\right|_{\hat{x}_{k-1|k-1},u_k}dt\right)^T+\\ \left(\left.\frac{\partial f}{\partial u}\right|_{\hat{x}_{k-1|k-1},u_k}dt\right)Q_k\left(\left.\frac{\partial f}{\partial u}\right|_{\hat{x}_{k-1|k-1},u_k}dt\right)^T\end{pmatrix}\times\left(\left.\frac{\partial h}{\partial x}\right|_{\hat{x}_{k|k-1}}\right)^T\ldots\right)^{-1}\ldots$$

$$\times\left(H_k\begin{pmatrix}\left(I+\left.\frac{\partial f}{\partial x}\right|_{\hat{x}_{k-1|k-1},u_k}dt\right)P_{k-1|k-1}\left(I+\left.\frac{\partial f}{\partial x}\right|_{\hat{x}_{k-1|k-1},u_k}dt\right)^T+\\ \left(\left.\frac{\partial f}{\partial u}\right|_{\hat{x}_{k-1|k-1},u_k}dt\right)Q_k\left(\left.\frac{\partial f}{\partial u}\right|_{\hat{x}_{k-1|k-1},u_k}dt\right)^T\end{pmatrix}H_k^T+R_k\right)\ldots$$

$$\times\left(\left.\frac{\partial h}{\partial x}\right|_{\hat{x}_{k|k-1}}\right)\times\begin{pmatrix}\left(I+\left.\frac{\partial f}{\partial x}\right|_{\hat{x}_{k-1|k-1},u_k}dt\right)P_{k-1|k-1}\left(I+\left.\frac{\partial f}{\partial x}\right|_{\hat{x}_{k-1|k-1},u_k}dt\right)^T+\\ \left(\left.\frac{\partial f}{\partial u}\right|_{\hat{x}_{k-1|k-1},u_k}dt\right)Q_k\left(\left.\frac{\partial f}{\partial u}\right|_{\hat{x}_{k-1|k-1},u_k}dt\right)^T\end{pmatrix}\times$$

$$\left(H_k \left(\left(I + \frac{\partial f}{\partial x}\Big|_{\hat{x}_{k-1|k-1},u_k} dt \right) P_{k-1|k-1} \left(I + \frac{\partial f}{\partial x}\Big|_{\hat{x}_{k-1|k-1},u_k} dt \right)^T + \left(\frac{\partial f}{\partial u}\Big|_{\hat{x}_{k-1|k-1},u_k} dt \right) Q_k \left(\frac{\partial f}{\partial u}\Big|_{\hat{x}_{k-1|k-1},u_k} dt \right)^T \right) H_k^T + R_k \right). \tag{22}$$

Having the covariance matrices of each agent and using the Equations (18), (19), and (20), the total covariance matrix is obtained as a function of the positions of the three agents. Therefore, the optimization problem was defined as follows:

"It is desirable to position the agents at any time such that the determinant or trace of total covariance matrix minimizes."

$$min_{X_f \in [x_1, y_1, x_2, y_2, x_3, y_3]} \begin{cases} f(X_f) = determinant(P_{CNS}) \\ \text{or } f(X_f) = trace(P_{CNS}). \end{cases} \tag{23}$$

Accordingly, Newton's method will be used to achieve this goal. Using this method, in each step, the next best place of agents is expected to minimize the optimality criterion. This movement towards minimization will be achieved through the steps that will lead to the next best place for minimization of the determinant or trace of the matrix P_{CNS}:

$$X_f^{k+1} = X_f^k + \delta^k, \tag{24}$$

where δ^k will be a function of the jacobian and hessian of the covariance matrix and it will be obtained as follows (Fletcher, 2000):

$$\delta^k = -\left(G^k\right)^{-1} g^k, \tag{25}$$

where, g^k and G^k are jacobian and hessian of $f\left(X_f^k\right)$ respectively:

$$g^k = \nabla f\left(X_f^k\right) \ , \ G^k = \nabla^2 f\left(X_f^k\right). \tag{26}$$

Therefore, if the Jacobin and Hessian of the matrix $f\left(X_f^k\right)$ can be obtained simultaneously, it can be expected that the optimal formation will be formed in the mission.

6. Simulation

In this section, the presented algorithm will be simulated. The simulation was performed in two modes using actual data for the cooperative navigation algorithm and modeled data for the optimal formation algorithm.

6.1. Offline simulation with actual data

Real IMU was used to validate the cooperative navigation algorithm. The output of two micro-electromechanical system (MEMS) IMU, which is stationary at a constant distance from each other in parallel, is used for navigation for two minutes. Using this data and inaccurate alignment, navigation has been simulated with and without CNS. These sensors are GY-87 and GY-955. In order to use the CNS algorithm better, a reference point is also considered as a virtual IMU with ideal navigation (i.e., the error of the navigation variables is zero). Figure 1 shows the layout of these IMUs, which is read through an ARDUINO board.

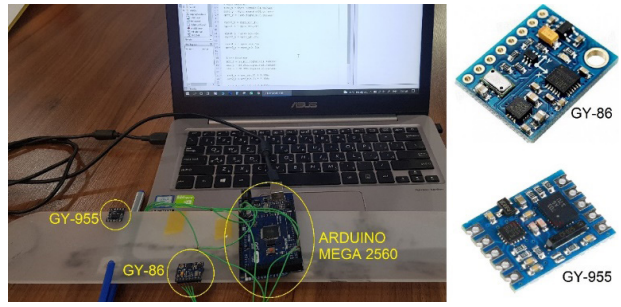

Figure 1. IMUs GY-955 and GY-86

In addition, Figure 2 shows the error of the IMU GY-86 and the IMU GY-955 navigation variables when the CNS is not used.

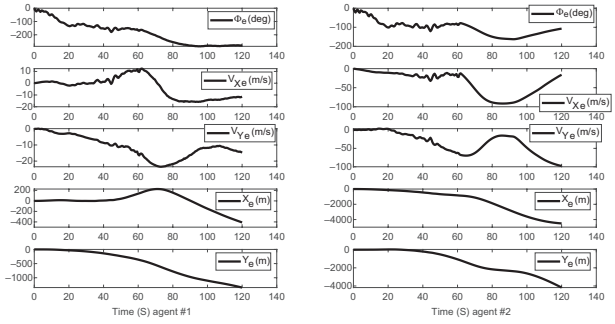

Figure 2. State navigation error for IMU GY-86 (left) & State navigation error for IMU GY-955 (right) (No CNC)

In other simulations, the same outputs are entered into the CNS algorithm. Figure 3 shows the error of the IMU GY-86 navigation variables and the error of the IMU GY-955 navigation variables when the CNS was used. It can be seen that the amount of all errors is less than before.

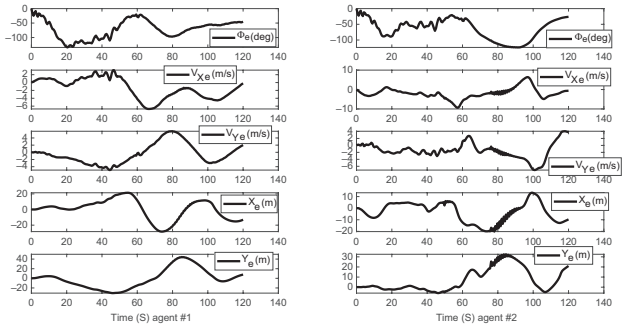

Figure 3. State navigation error for IMU GY-86 (left) & State navigation error for IMU GY-955 (right) (Via CNC)

The data of the Table 2 show that the error is very high when each of the IMUs navigates separately, while the error is significantly reduced when the same data is entered into the CNS algorithm.

Table 2. Comparison of the error of IMU navigation variables

States Error		Without CNS	With CNS
IMU GY-86	j Error (deg)	279.2998	45.449
	v_x Error (m/s)	11.4931	0.19547
	v_y Error (m/s)	14.7345	–2.0193
	x Error (m)	410.1866	13.063
	y Error (m)	1345.6542	–7.9911
	***xy* MSE (m)**	**175.7176**	**6.9324**
	***xy* Final Error (m)**	**1406.783**	**15.3134**
IMU GY-955	j Error (deg)	107.0979	25.9609
	v_x Error (m/s)	15.6274	0.64993
	v_y Error (m/s)	97.8021	–3.7261
	x Error (m)	4480.2852	9.699
	y Error (m)	4202.6616	–20.8414
	***xy* MSE (m)**	**684.7162**	**4.276**
	***xy* Final Error (m)**	**6142.9082**	**22.9877**
Total Error (m)		**7549.6914**	**38.301**
Percentage Reduction		–	**99.49%**

6.2. Simulation for optimal makeup

In another simulation, three agents which have a MEMS navigation system are considered, such that the accuracy of one of them is more than the others. These agents move freely on the 2D space due to the acceleration applied to them. The mission for these agents is to move from one position to another, according to Table 3, and the features of the sensors intended for the agents are presented in the same table.

Table 3. Initial and desired position and inertia navigation sensor error of agents

Agent	Initial Position $[x_0,y_0]$	Desired Position $[x_d,y_d]$	Accelerometer Error (g)	Gyro Error (°/hr)
Agent #1	[10; 0]	[300; 90]	0.01	0.01
Agent #2	[0; 10]	[360; 120]	0.3	0.3
Agent #3	[0; 0]	[330; 150]	0.3	0.3

According to the simulation, the output of the inertial navigation system for the agents' path to the desired positions is shown in Figure 4. In this simulation, each agent uses only its navigation system and does not use cooperative navigation.

Through the path of the agents, moving from the initial position to the desired position, which is achieved due to the control accelerations, the errors of the navigation variables are plotted as diagrams in Figure 5. These diagrams show that the navigation error increases over time and the navigation error of agents #2 and #3 is greater than that of agent #1, and the reason is that the sensors selected for agents #2 and #3 are more inaccurate than that of agent #1.

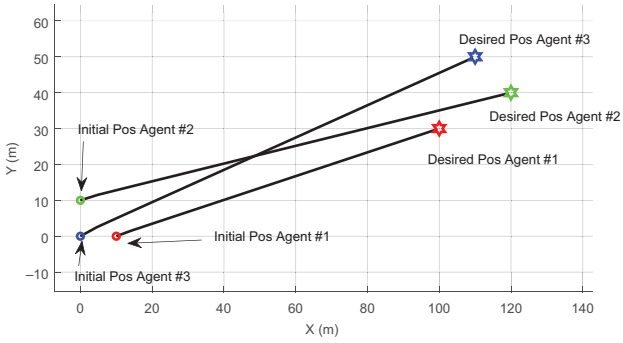

Figure 4. Agents' path (No CNC – No Formation)

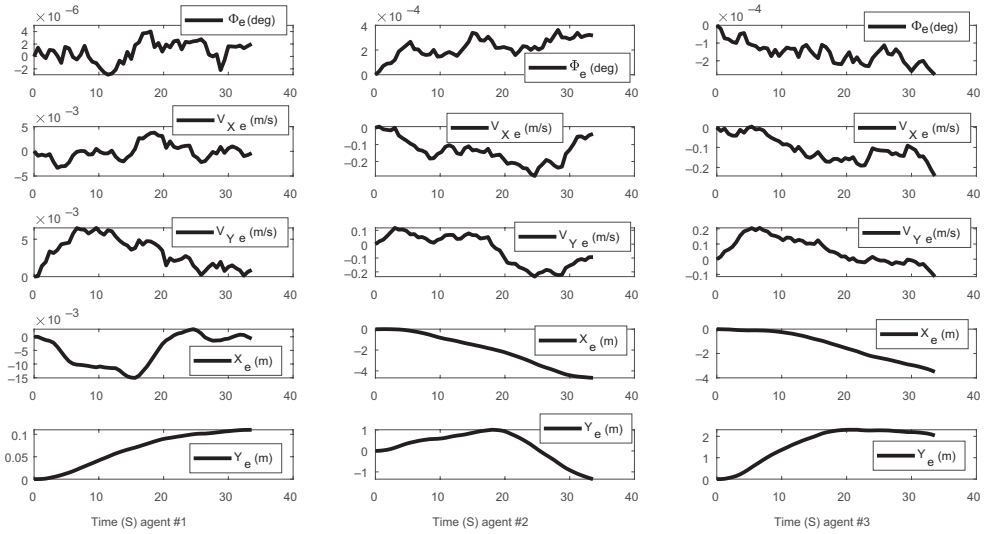

Figure 5. State navigation error for agent #1 (left), agent #2 (middle) and agent #3 (right) (No CNC – No Formation)

In another simulation, the same motion scenario was run using CNS, the results of which are presented in Figure 6 and Figure 7. In these figures, it is clear that the error of the navigation states variable has been reduced to the extent that the error of all three agents is almost in the same range.

In the third simulation, in addition to CNS, the optimal formation was also considered such that along the way, the agents, in addition to going to the final desired locations, also tended to form the formation to minimize the trace of the total covariance matrix.

In order to have a balance between going towards the desired formation and going towards the final location, two types of control acceleration have been considered: one of which leads the agent to the final desired location and the other to the desired formation. Equation (27) shows the combination of these control accelerations:

$$\vec{a} = \left(1 - W_F\right)\vec{a}_c + W_F\vec{a}_f \,, \tag{27}$$

where $\vec{a}_c$ is the control acceleration to reach the final position, $\vec{a}_f$ is the control acceleration to achieve the optimal formation, and w is also the weighting factor between these two accelerations such that its value varies between 0 and 1 and it proposes to be defined as follows:

$$W_F = X_e / X_d \,, \tag{28}$$

where X_e is the error position of the agents with respect to the final goals, and X_d the final goals they must reach. Based on Equation (28), it is clear that in the beginning, when the distance between the agents and the final goals is significant, w is close to 1. Gradually, as the agents get closer to the final goals, the w will be close to 0. This process of change means that in the beginning, achieving the optimal formation is more important because with better formation, the error will be reduced, and eventually achieving the goals will be more important because the mission was to reach the final locations. Moreover, if the formation has a high coefficient, the control accelerations will prevent the agents from reaching the final goals. Figure 8 shows the trend of changes in this factor over time. Figure 9 also shows the path of the agents to reach the final goals. In this figure, the path is different from the paths shown in Figure 4 and Figure 6 because the agents tend to form the optimal formation. In fact, in addition to trying to reach the final desired locations, agents try to form the geometry at any time to reduce the total navigation error in the CNS algorithm.

Table 4 represents the comparison of these three simulations. It is clear that when the CNS is not used, each agent has outputs with different accuracy according to the accuracy of its navigation sensors, but when the CNS is used, the navigation error of all agents is almost in the same range. Overall, navigation accuracy has improved by about 43%. For example, agent #3 has a position error of about 4.8 meters when the CNS is not used but a position error of about 2.4 meters when CNS is used. This improvement is also achieved for agent #2, which has increased from a position error of about 5.4 meters to an error of

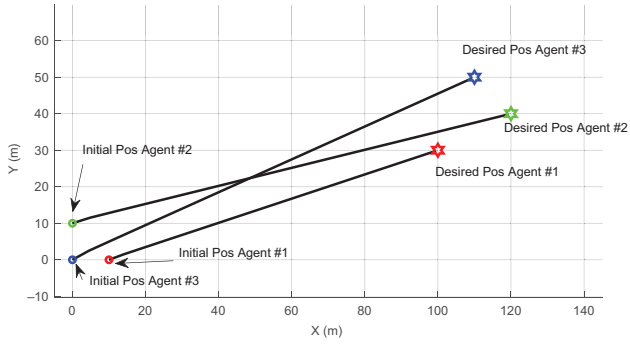

Figure 6. Agents' path (Via CNC – No Formation)

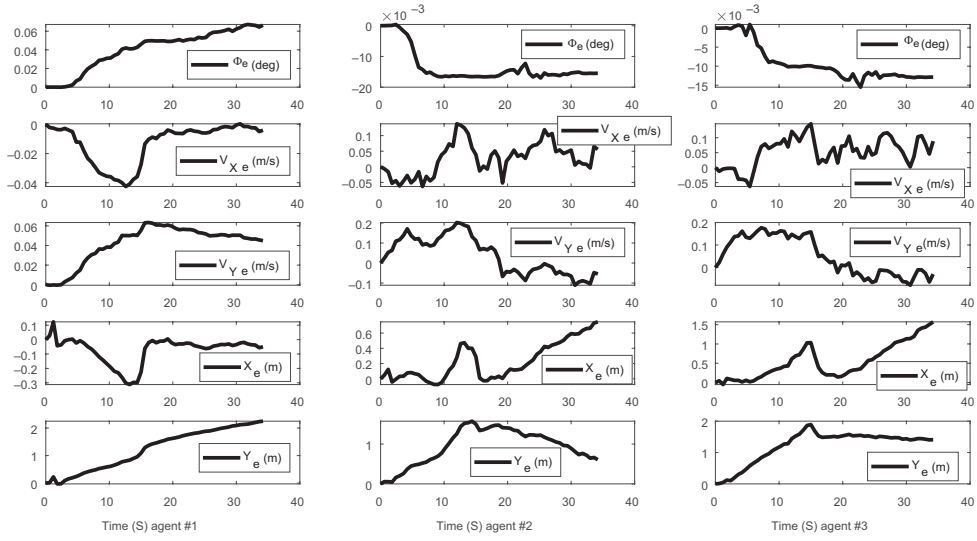

Figure 7. State navigation error for agent #1 (left), agent #2 (middle) and agent #3 (right) (Via CNC – No Formation)

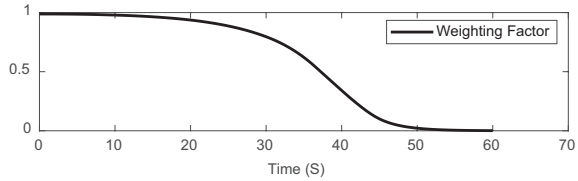

Figure 8. Weighting factor

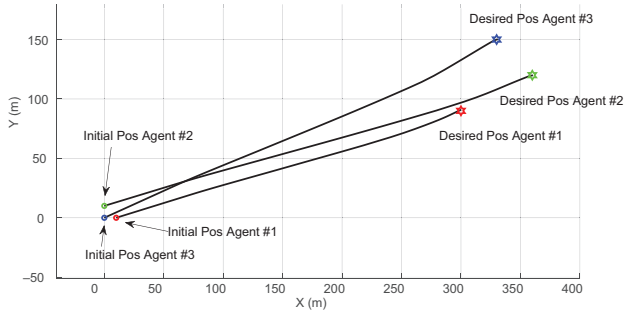

Figure 9. Agents' path (Via CNC – Via Formation)

about 1 meter, but, in agent #1, the issue is different, and it seems the position error of this agent has increased. One of the issues with CNS is that just like a precision navigation system which has a positive effect on a less accurate navigation system, a less accurate navigation system will have a negative effect on a more accurate navigation system. Therefore, the error of agent #1 increased. Also, when the optimal formation algorithm is used to minimize the trace of the total covariance matrix, the navigation error further reduces in addition to the CNS. This error reduction is about 79% less than when there is no algorithm.

Conclusions

Improving the performance of cooperative navigation by adding the relative distances between agents as well as the proper formation is investigated in this paper. The former method was evaluated through various simulations and experimental tests using two real agents equipped with INS. Experimental results show that the navigation errors would significantly reduce, such that the total position error reduced from 7550 m to 38.3 m. In the simulation, cooperative navigation was simulated considering the relative distance between three agents with inertial navigation systems with different accuracy. The result was interesting: using CNS, the total navigation accuracy increases, and all the navigation systems reach the same range of precision. The position error of the agents without considering CNS became 0.11 m, 5.48 m, and 4.82 m, respectively, but considering CNS, the errors became 2.38 m, 1.06 m, and 2.43 m, respectively. Therefore, it was seen a 43.68% improvement in navigation performance. In addition, applying the optimal formation caused the reduction of

Table 4. Comparison of error of agents' navigation in three simulations

States Error		Without CNS and Formation	With CNS	With CNS and Formation
Agent #1	φ Error (deg)	–1.7394e-05	–6.7095e-02	–4.9713e-02
	v_x Error (m/s)	–4.3141e-03	–5.2514e-03	–8.2655e-03
	v_y Error (m/s)	–6.0243e-03	–5.9682e-02	–1.2583e-02
	x Error (m)	–5.9791e-03	8.9323e-03	1.5645e-01
	y Error (m)	–1.1238e-01	–2.3762	–6.1521e-01
	***xy* MSE (m)**	**1.9575e-02**	**4.0855e-01**	**1.0816e-01**
	***xy* Final Error (m)**	**1.1254e-01**	**2.3762**	**6.3479e-01**
Agent #2	φ Error (deg)	–2.7147e-05	1.8343e-02	4.6838e-03
	v_x Error (m/s)	9.4365e-02	–1.0703e-01	–1.1658e-01
	v_y Error (m/s)	–6.5613e-02	6.2130e-02	4.0756e-02
	x Error (m)	3.8851	–9.8628e-01	–4.7185e-01
	y Error (m)	–3.8664	–3.9276e-01	4.3759e-01
	***xy* MSE (m)**	**9.9580e-01**	**3.3156e-01**	**1.1734e-01**
	***xy* Final Error (m)**	**5.4812**	**1.0616**	**6.4353e-01**
Agent #3	φ Error (deg)	–1.3953e-04	1.3013e-02	8.8601e-03
	v_x Error (m/s)	–3.2008e-02	–1.3173e-01	–8.3787e-02
	v_y Error (m/s)	–5.6724e-02	2.7972e-02	7.9591e-02
	x Error (m)	–1.0213	–1.9941	–9.0905e-01
	y Error (m)	–4.7166	–1.3889	1.4040e-02
	***xy* MSE (m)**	**8.8573e-01**	**4.8294e-01**	**1.4211e-01**
	***xy* Final Error (m)**	**4.8259**	**2.4301**	**9.0916e-01**
Total Error (m)		**10.4196**	**5.8679**	**2.19**
Percentage Reduction		–	**43.68%**	**78.98%**

navigation error more than before, such that in this case, the position error for the agents was 0.62 m, 0.64 m, and 0.91 m, respectively, which showed a 78.98% improvement in navigation performance. An advantage of this method was that without using any aided navigation system (e.g., GPS), the navigation accuracy increased, which means a reduction in the cost of navigation equipment. Since achieving suitable formation requires considerable computing, other computational methods can be attempted in the future. It is even possible to provide other optimization criteria for the formation to reduce the navigation error further. For example, the Cramer-Rao lower bound (CRLB) criterion can be considered as the optimality criterion. Movement Formation can also be based on other goals. For example, the agents can perform better in simultaneous localization and mapping (SLAM).

Disclosure statement

Authors have no competing interests from other parties.

References

Causa, F., Vetrella, A. R., Fasano, G., & Accardo, D. (2018, 23–26 April). Multi-UAV formation geometries for cooperative navigation in GNSS-challenging Environments. In *ION Position, Location and Navigation Symposium (PLANS)*. Monterey, CA, USA. IEEE. https://doi.org/10.1109/PLANS.2018.8373453

Chen, J., Wang, X., Shao, X., & Duan, D. (2010, 8–10 June). An integrated Relative Navigation system using GPS/VISNAV for ultra-close spacecraft formation flying. In *3rd International Symposium on Systems and Control in Aeronautics and Astronautics.* The Institute of Electrical and Electronics Engineers. https://doi.org/10.1109/ISSCAA.2010.5633067

Chen, M., Xiong, Z., Liu, J., Wang, R., & Xiong, J. (2020, June 22). Cooperative navigation of unmanned aerial vehicle swarm based on cooperative dilution of precision. *International Journal of Advanced Robotic Systems, 17*(3). https://doi.org/10.1177/1729881420932717

Cledat, E., & Cucci, D. A. (2017, 4–7 September). Mapping GNSS restricted environments with a drone tandem and indirect position control. In *ISPRS Annals of the Photogrammetry, Remote Sensing and Spatial Information Sciences, IV-2/W3* (pp. 1–7). Bonn, Germany. https://doi.org/10.5194/isprs-annals-IV-2-W3-1-2017

Cutler, M., Michini, B., & How, J. P. (2013). Lightweight infrared sensing for relative navigation of quadrotors. In *International Conference on Unmanned Aircraft Systems (ICUAS).* IEEE. https://doi.org/10.1109/ICUAS.2013.6564807

Faghihinia, A., Amiri Atashgah, M. A., & Dehghan, S. M. (2021). Analytical expression for uncertainty propagation of aerial cooperative navigation. *Aviation, 25*(1), 10–21. https://doi.org/10.3846/aviation.2021.13420

Fletcher, R. (2000). *Practical methods of optimization* (2nd ed.). John Wiley and Sons Ltd. https://doi.org/10.1002/9781118723203

Fosbury, A. M., & Crassidis, J. L. (2008). Optimal trajectory determination for increased relative navigation observability of air vehicles. In *American Institute of Aeronautics and Astronautics Guidance, Navigation and Control Conference and Exhibit* (pp. 1–19). Honolulu, Hawaii. https://doi.org/10.2514/6.2008-6648

Guo, K. (4 December, 2018). *Ultra-wideband-based navigation for unmanned aerial vehicles.* Nanyang Technological University.

Hong, Y., & Simon, D. (2017, August 6–9). Relative navigation of non-cooperative space target based on multiple cooperative space robots. In *ASME 2017 International Design Engineering Technical Conferences and Computers and Information in Engineering Conference IDETC/CIE 2017*. Cleveland, Ohio, USA. http://proceedings.asmedigitalcollection.asme.org/

Jin, Y., Zhang, Y., Yuan, J., & Zhang, X. (12–17 May, 2019). Efficient Multi-agent cooperative navigation in unknown environments with interlaced deep reinforcement learning. In *ICASSP 2019 – 2019 IEEE International Conference on Acoustics, Speech and Signal Processing (ICASSP).* Brighton, United Kingdom. https://doi.org/10.1109/ICASSP.2019.8682555

Khambhaita, H., & Alami, R. (28 November, 2019). Viewing robot navigation in human environment as a cooperative activity. *Robotics Research, 10*, 285–300. https://doi.org/10.1007/978-3-030-28619-4_25

Lee, J., Kang, D. E., & Park, S. Y. (2018). Relative navigation with laser-based intermittent measurement for formation flying satellites. *International Journal of Aerospace and Mechanical Engineering, 12*(2), 73–77.

Martin, S. M. (2011, May 9). *Closely coupled GPS/INS relative positioning for automated vehicle*. Auburn University.

Mokhtarzadeh, H., & Gebre-Egziabher, D. (2016). Performance of networked dead reckoning navigation system. *IEEE Transactions on Aerospace and Electronic Systems, 52*(5), 2539–2553. https://doi.org/10.1109/TAES.2016.150180

Montenbruck, O., Ebinuma, T., Lightsey, E. G., & Leung, S. (2002, October). A real-time kinematic GPS sensor for spacecraft relative navigation. *Aerospace Science and Technology, 6*(6), 435–449. https://doi.org/10.1016/S1270-9638(02)01185-9

Noureldin, A., Karamat, T., & Georgy, J. (2013). *Fundamentals of inertial navigation, satellite-based positioning and their integration.* Springer. https://doi.org/10.1007/978-3-642-30466-8

Roumeliotis, S. I., & Bekey, G. A. (2002). Distributed multirobot localization. *IEEE Transactions on Robotics and Automation, 18*(5), 781–795. https://doi.org/10.1109/TRA.2002.803461

Rutkowski, A. J., Barnes, J. E., & Smith, A. T. (2016). Path planning for optimal cooperative navigation. In *2016 IEEE/ION Position, Location and Navigation Symposium (PLANS).* IEEE. https://doi.org/10.1109/PLANS.2016.7479721

Sanderson, A. C. (1998). A distributed algorithm for cooperative navigation among multiple mobile robots. *Advanced Robotics, 12*, 335–349. https://doi.org/10.1163/156855398X00235

Sheikh, S. I., Ray, P. S., Weiner, K., Wolff, M. T., & Wood, K. S. (2007). Relative navigation of spacecraft utilizing bright, aperiodic celestial sources. In *63rd Annual Meeting of the Institute of Navigation* (pp. 444–453). The Institute of Navigation.

Sivaneri, V. O., & Gross, J. N. (2017, December). UGV-to-UAV cooperative ranging for robust navigation in GNSS-challenged environments. *Aerospace Science and Technology, 71*, 245–255. https://doi.org/10.1016/j.ast.2017.09.024

Summerfield, N. S., Deokar, A. V., Xu, M., & Zhu, W. (2020, 6 February). Should drivers cooperate? Performance evaluation of cooperative navigation on simulated road networks using network DEA. *Journal of the Operational Research Society, 72*. https://doi.org/10.1080/01605682.2019.1700766

Thomason, J., Murray, M., Cakmak, M., & Zettlemoyer, L. (2020). Vision-and-dialog navigation. In *Conference on Robot Learning, PMLR.* ArXiv.

Vetrella, A. R., Fasano, G., & Accardo, D. (2016, 7–10 June). Cooperative navigation in GPS-Challenging environments

exploiting position broadcast and vision-based tracking. In *2016 International Conference on Unmanned Aircraft Systems (ICUAS)*. Arlington, VA USA. IEEE. https://doi.org/10.1109/ICUAS.2016.7502647

Vetrella, A. R., Opromolla, R., Fasano, G., Accardo, D., & Grassi, M. (2017, 9–13 January). Autonomous flight in GPS-Challenging environments exploiting multi-UAV cooperation and vision-aided navigation. In *AIAA SciTech Forum*. AIAA Information Systems-AIAA Infotech @ Aerospace. https://doi.org/10.2514/6.2017-0879

Vetrella, A. R., Fasano, G., & Accardo, D. (2018). Attitude estimation for cooperating UAVs based on tight integration of GNSS and vision measurements. *Aerospace Science and Technology*, *84*, 966–979. https://doi.org/10.1016/j.ast.2018.11.032

Wang, X. (2011, April). Improved adaptive filter with application to relative navigation. *GPS Solutions, 15*(2), 121–128. https://doi.org/10.1007/s10291-010-0175-7

Wang, X., Gong, D., Xu, L., Shao, X., & Duan, D. (2011a, June–July). Laser radar based relative navigation using improved adaptive Huber filter. *Acta Astronautica, 68*(11–12), 1872–1880. https://doi.org/10.1016/j.actaastro.2011.01.002

Wang, X., Shao, X., Gong, D., & Duan, D. (2011b, April). GPS/VISNAV integrated relative navigation and attitude determination system for ultra-close spacecraft formation flying. *Journal of Systems Engineering and Electronics, 22*(2), 283–291. https://doi.org/10.3969/j.issn.1004-4132.2011.02.015